

ARTICLES

Magnetophotoselection in the Spin-Polarized Triplet State Radical-Ion Pair Formed in the Photo-Induced Solvent-Mediated Electron Transfer Reaction from *N,N*-Diethylaniline to Xanthone in Viscous SolutionAsako Ishigaki,^{†,‡} Yasuhiro Kobori,[§] and Hisao Murai^{*,§}*Graduate School of Science and Technology, Shizuoka University, Shizuoka, Japan, and Department of Chemistry, Faculty of Science, Shizuoka University, Shizuoka, Japan**Received: August 8, 2008; Revised Manuscript Received: November 18, 2008*

The triplet state radical-ion pair (RIP) formed in the photolysis of xanthone (Xn) and *N,N*-diethylaniline (DEA) in a highly viscous mixtures of 2-propanol and cyclohexanol was studied by time-resolved ESR. As the viscosity of the mixed solution increases, the spectrum reveals a magnetic dipole–dipole interaction in the triplet state of the RIP. Immediately after laser photolysis, the spin-polarized RIP spectrum exhibits magnetophotoselection (MPS). This suggests that the electron transfer (ET) reaction is faster than the longitudinal relaxation of the excited triplet state of Xn ($^3\text{Xn}^*$) or much faster than the tumbling motion of $^3\text{Xn}^*$. The former mechanism is likely under the conditions employed. Indeed, a huge RIP-cored aggregation is quickly formed with solvent molecules which obstruct the free revolution of the RIP. The MPS spectra also indicate that only the molecules closely located react by the solvent-mediated ET.

Introduction

Photoinduced electron transfer (ET) reaction of substances produces a transient radical-ion pair (RIP) immediately after excitation in solution. Some geminately formed RIPs are consumed from one of the spin multiplet states immediately after birth and other RIPs diffuse apart in the solution. The separated free radical ions reencounter to form a free pair RIP. The subsequent reaction depends on the spin multiplicity of these RIP. Therefore, spin chemical investigations of photoinduced ET reaction can provide very important information.

In general, the RIP formed in the photolysis survives only for a few tens of nanoseconds or less in homogeneous polar solution at room temperature, because of the weak Coulomb interaction and fast diffusion. A decade ago, a magnetic field effect on the photo reaction of xanthone (Xn) and *N,N*-diethylaniline (DEA) in 2-propanol was reported by Igarashi et al.¹ Their data imply the formation of a long-lived RIP in this particular system in which photoinduced ET reaction from DEA to the excited triplet state of Xn ($^3\text{Xn}^*$) takes place. The time-resolved photoconductivity detected magnetic resonance (PCD-MR) method (one of a group of reaction yield detected magnetic resonance (RYDMR) methods) was developed by Murai et al.^{2,3} and was used to confirm the long RIP lifetime in this reaction. The lifetime of the RIP was determined to be 180 ns,^{4–6} and the formation of a RIP networked with solvent molecules was suggested. Contrary to this model, Gorelik et al. reported a theoretical approach to this system in a homogeneous environment employing an integral encounter theory.⁷ Although the calculation, which assumed no local inhomogeneity, showed

fairly good agreement with the spectral shape at late times after photolysis, it did not reproduce the spectrum in the early time region. Recently, we reported the time-resolved ESR (tr-ESR) study of the long-lived RIP in 2-propanol and provided more precise information about the long-lived nature of this particular RIP.⁸ In ordinary liquid solution, the spin dipole–dipole (d–d) interaction of an intermediate RIP is averaged to zero, and the d–d interaction cannot be observed. However, the interaction is responsible for spin relaxation through the tumbling motion of the RIP. If the d–d interaction can be observed in rigid or very viscous media, it can provide detailed additional information about the RIP.

In the last few decades, magnetophotoselection (MPS) has been reported for photolysis reactions employing polarized light in rigid media. Examples include azides and nitrens derived from anthracene⁹ and saphyrin dication¹⁰ among others.^{11–16} MPS is useful for determination of the molecular orientation, the configuration efficiency of energy transfer and polarized reactions in photochemistry. Although many of the reported experiments were carried out under frozen and low temperature conditions, the d–d interaction is also likely to be observed in very viscous solution at room temperature.

In the present paper, we present a MPS study of the long-lived RIP formed in the Xn and DEA system in highly viscous solution, in order to clarify the formation mechanism of the RIP, its structure and its spin dynamics.

Experimental Section

Guaranteed reagents of Xn, 2-propanol, and cyclohexanol provided by Wako Pure Chemical, and DEA by Kanto Chemical were used as received. Solvents used were 2-propanol, cyclohexanol and mixture of 2-propanol and cyclohexanol. The concentrations of Xn and DEA were 3.0×10^{-2} M ($\text{mol} \cdot \text{dm}^{-3}$)

* Corresponding author.

[†] Graduate School of Science and Technology, Shizuoka University.

[‡] Japan Society for the Promotion of Science Fellow.

[§] Department of Chemistry, Faculty of Science, Shizuoka University.

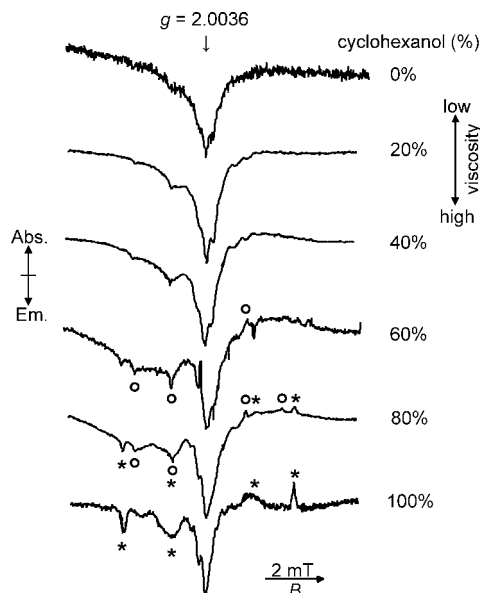
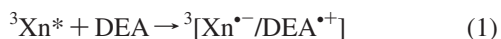


Figure 1. Tr-ESR spectra observed at 400–500 ns after the laser photolysis for mixtures of 2-propanol and cyclohexanol of varying composition. The amplitude direction of the linearly polarized laser light is perpendicular to the magnet field ($B_0 \perp E$). ○ and * show the neutral DEA radical and cyclohexanol radical, respectively.

and 2.0×10^{-2} M, respectively, in most experiments. The sample solution was deoxygenated by bubbling with nitrogen gas and made to flow through a flat quartz cell installed in an X-band ESR cavity at room temperature (*ca.* 298 K). The sample was excited with the third harmonic of a pulsed Nd:YAG laser (Continuum Minilite; $\lambda = 355$ nm; 10 Hz), which selectively photoexcites the Xn molecules. Linearly polarized laser light was arranged parallel or perpendicular to the ESR magnetic field for the MPS experiments. An ESR spectrometer (Varian E-112) was used with a minor modification for the time-resolved measurement.^{17,18} The microwave signal reflected from the ESR resonator was boosted by a wide band amplifier (NF Electronics Instruments BX-31) and transferred to a digital oscilloscope (LeCroy 9430), triggered by a pin-photo diode, to record the time-evolution. In the included figures, the microwave absorption and emission are abbreviated by **A** and **E** (**a** and **e** for weak signals), respectively. The dielectric constant of the solution was measured by the combination of a dielectric measurement cell (Hewlett-Packard 16452A) and an impedance meter (NF Electronic Instruments 2322). A Toki RE80 viscosity meter was used to determine the viscosity of the solvents.

Results and Discussion

The formation of a long-lived RIP by photoinduced ET reaction of Xn and DEA in 2-propanol has been reported^{4–6,8} as follows:



where the square brackets show the RIP.

Spectral Change by the Mixing Ratio of 2-Propanol and Cyclohexanol. Addition of cyclohexanol to this system causes tr-ESR spectrum to change dramatically as shown in Figure 1. Table 1 shows the viscosity (η), relative permittivity (ϵ_r) and diffusion-controlled rate constant (k_{diff})¹⁹ of the mixture of 2-propanol and cyclohexanol for different solvent mixing ratios. Increasing the proportion of cyclohexanol in the mixture drastically changes η , but has little effect on ϵ_r . The emissive spectrum observed without cyclohexanol is almost completely

due to the Xn anion free radicals ($g = 2.0036$) as reported previously.⁸ Addition of cyclohexanol to the solution, in the concentration range of 40%–80%, produces a broad **E/A** (**E** at lower field and **A** at higher field) pattern alongside the center emissive component as shown in the figure. Some weak peaks superimposed over a wider field range (indicated by open circles and asterisks) are also observed. These spectra are the minor byproducts of whole reaction; the open circles and the asterisks are assigned to the neutral DEA radical ($a_\alpha(1) = 1.58$ mT, $a_\beta(3) = 2.03$ mT)²⁰ and the cyclohexanol radical,^{21–23} respectively. The broad **E/A** pattern observed over a wide spectral field range is due to the appearance of the spin d–d interaction of the triplet state RIP formed by the photoinduced ET reaction. The appearance of the triplet state is due to the restrained tumbling motion of the RIP in highly viscous conditions. A large cluster-like or huge aggregate structure involving solvent molecules may be proposed to explain the obstruction to free rotation. The spin polarization of the RIP may be explained by the transfer of spin polarization from ${}^3\text{Xn}^*$ with spin angular momentum conserved.

A drastic spectral change is observed for photolysis in pure cyclohexanol. The broad **E/A** component disappears even though ET might be anticipated under these conditions. This spectrum is readily assigned to the cyclohexanol radical and Xn ketyl radical.^{21–23} Therefore, the hydrogen abstraction reaction by ${}^3\text{Xn}^*$ from cyclohexanol becomes more rapid than the ET reaction with DEA due to the high concentration of cyclohexanol and slow diffusion. This result also suggests that 2-propanol may assist both the ET reaction and the formation of the huge aggregate RIP.

Observation of MPS Spectra Showing the Spin Dipole–dipole Interaction. Parts a and b of Figure 2 show spectra from the MPS experiment performed in 60% cyclohexanol solution, where a) the plane of linearly polarized laser light is parallel to the magnet field ($B_0 \parallel E$), and b) the plane is perpendicular to the magnetic field ($B_0 \perp E$). Both spectra gradually grow and reveal nearly the same MPS free pattern at 400–500 ns. The growth of these spectra at late time is likely due to another polarization mechanism, such as chemical depletion of the RIP via S–T₀ mixing, but we do not discuss it in this paper. If the MPS is due to the transfer of the spin polarization from ${}^3\text{Xn}^*$ to the RIP as mentioned above, analysis of the MPS may clarify the dynamics of ET during the initial stage of the reaction. All the spectra show emissively biased components. The total **E** pattern is due to the influence of the spin polarization of the ${}^3\text{Xn}^*$ under the magnetic field of the ESR machine.^{24,25} The spectra at 100–200 ns after laser excitation reveal a different spin polarization pattern as shown in Figure 3, which corresponds to the expanded central region of the spectra in Figure 2. To analyze the spectra for the spin d–d interaction of randomly oriented RIPs, a point d–d approximation is used, where four canonical points appear. The zero field splitting (ZFS) parameters D and E of the RIP are negative and zero, respectively. The outside and inside points (indicated by asterisks) correspond to the principal Z axis and the (X, Y) axes, perpendicular to the Z axis, respectively. Hereafter, we will use X' , Y' , and Z' for the principal axes of this RIP. To analyze the polarization pattern of the RIP, we used these four points and a ZFS parameter (D) of -7.0 mT, estimated by the simulation of the spectra (shown in later discussion). The relation between the distance (d) between electron spins and D under the conditions of frozen or restrained movement is given as

TABLE 1: Viscosity and Relative Permittivity of Mixed Solvents (298 K)^a

volume of cyclohexanol in solvent (%)	viscosity (η) (cP)	relative permittivity (ϵ_r)	diffusion-controlled rate constant (k_{diff})/10 ⁸ (M ⁻¹ S ⁻¹)
0	1.89	19.2	45 ¹⁹
20	2.78	18.3	31
40	5.21	17.2	16
60	9.24	16.8	9.2
80	20.3	17.0	4.2
100	34.1	15.7	2.5

^a The k_{diff} is given as $k_{diff} = 8RT/2000\eta$, where R and T are the Boltzmann constant and temperature.

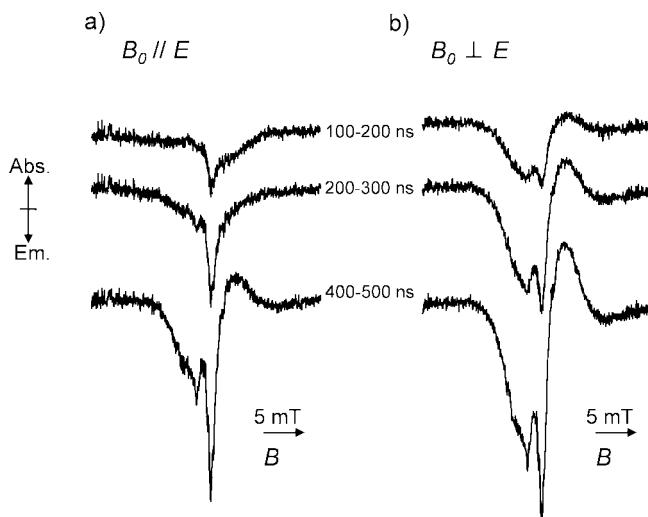


Figure 2. Tr-ESR spectra showing MPS observed for a solution containing 60% cyclohexanol. (a) The amplitude direction of the linearly polarized laser light is parallel to the magnet field ($B_0 \parallel E$). (b) The amplitude direction is perpendicular to the magnet field ($B_0 \perp E$).

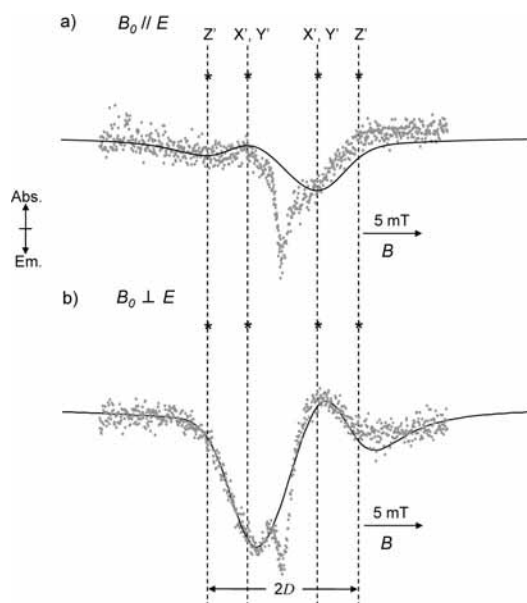


Figure 3. Expanded spectra of (a) $B_0 \parallel E$ and (b) $B_0 \perp E$ at 100–200 ns from Figure 2. The solid lines are the simulation calculated using the model of free molecular rotation where emissive TM is included with arbitrary weight (see text).

$$D = -\frac{3\mu_0(g\mu_B)^2}{2 \cdot 4\pi d^3} \quad (2)$$

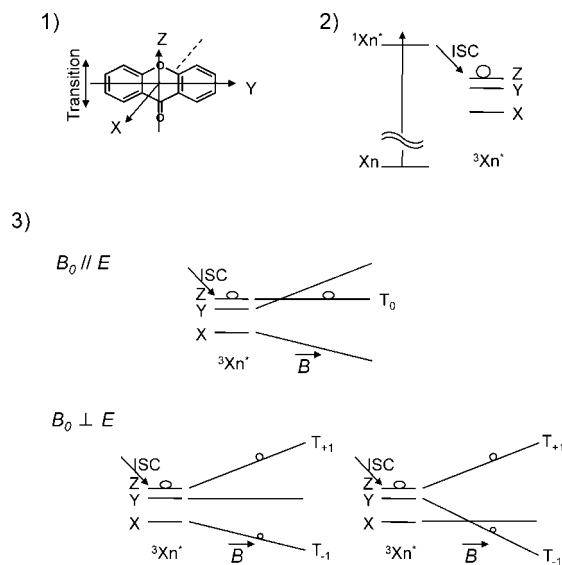


Figure 4. (1) Transition moment of excitation of Xn at 355 nm. (2) Intersystem crossing from $^1Xn^*$ to $^3Xn^*$. (3) Spin polarization of $^3Xn^*$ in the presence of a magnetic field in case of $B_0 \parallel E$ and $B_0 \perp E$.

Here g , μ_B and μ_0 are the electron g factor, Bohr magneton, and magnetic permeability, respectively.²⁶ According to eq(2) with $D = -7.0$ mT, d is determined to be 0.74 nm. This value agrees well with the approximate value of 0.6 nm reported in the previous paper,⁸ where the distance of two point spins is estimated as the shortest limit. It is noteworthy that the structure of the RIP is composed as a huge aggregate including the solvent molecules.

Mechanism of MPS Appearance. Here, let us consider the MPS spectra of the RIP at 100–200 ns. There are two possible mechanisms, depending upon the rigidity of the medium and the efficiency of the ET reaction: (I) a free molecular rotation model and (II) a restrained molecular motion model. Parts 1 and 2 of Figure 4 illustrate the transition moment of excitation from the ground-state to the lowest excited singlet state of Xn ($^1Xn^*$) at 355 nm.^{27,28} The principal axes of the ZFS of $^3Xn^*$ are defined according to reported papers^{29–31} as follows: the Z axis is parallel to the carbonyl direction, Y axis is perpendicular to Z axis in the molecular plane, and X axis is perpendicular to the molecular plane. The upper sublevel of $^3Xn^*$, Z, is actively populated by intersystem crossing (ISC) from $^1Xn^*$ due to the spin–orbit interaction while the lower two sublevels, X and Y, are unpopulated.

I. Free Molecular Rotation Model. In this model, the free rotation of $^3Xn^*$ is allowed during ET. The spin polarization of $^3Xn^*$ induced by the ISC is quantized to the direction of the ESR magnetic field depending upon the amplitude direction of the linearly polarized light relative to the field as shown in Figure 4–3. If the spin polarization of the laboratory frames is

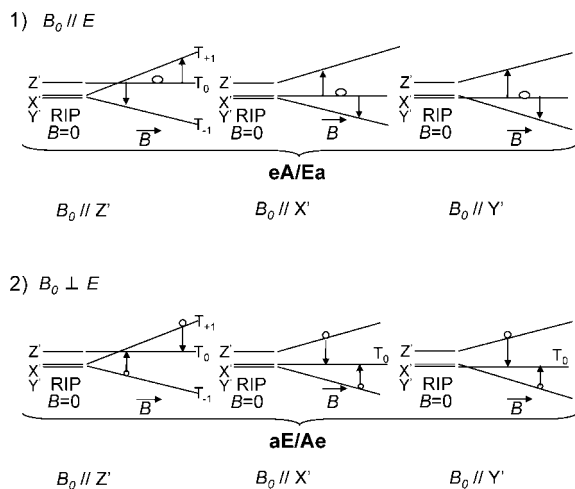


Figure 5. Parts 1 and 2 show the population of the spin sublevels of the RIP transferred from $^3\text{Xn}^*$ keeping the character of the T_0 state ($B_0 \parallel E$) and T_{+1} , T_{-1} states ($B_0 \perp E$), respectively. These diagrams also show the corresponding typical spin polarized spectral patterns.

conserved during the ET, the character of T_{+1} , T_0 , T_{-1} is transferred to the RIP even if the $^3\text{Xn}^*$ rotates freely. In case of $B_0 \parallel E$ where the Z axis is parallel to B_0 , the T_0 state of $^3\text{Xn}^*$ is most populated. Therefore, the population of the T_0 state is transferred to the RIP. Similarly, the T_{+1} and T_{-1} states are most populated in case of $B_0 \perp E$, and these populations are transferred to the RIP. The spectral patterns obtained for $B_0 \parallel E$ and $B_0 \perp E$ are $\mathbf{eA/Ea}$ and $\mathbf{aE/Ae}$, respectively as illustrated in Figure 5. Of course, for excitation using linearly polarized light, the most probable direction of the transition moment of the molecule is parallel to that of the polarized light. Therefore, the simple discussion above is possible. However, even molecules with transition moments aligned at an angle θ relative to the amplitude direction of the polarized light can be excited with the probability of $\cos^2 \theta$. This implies that the RIP formed by the ET between randomly oriented $^3\text{Xn}^*$ and DEA obtains overall \mathbf{E} spin polarization even in the case of $B_0 \parallel E$. Although the estimation of this TM-like spin polarization needs exact calculation (including the contribution of $\cos^2 \theta$), a population ratio of T_{+1} to T_0 state of 2 ($\rho_{+1}/\rho_0 = 2$) and a population of the T_{-1} state of zero ($\rho_{-1} = 0$) are temporarily assumed. The simulated spectra obtained by combining the spectral pattern calculated by the simple population transfer from T_0 or T_{+1} and T_{-1} states of $^3\text{Xn}^*$ to the RIP and that of emissive TM reproduce the observed spectra well, as shown in the Figure 3 where the T_2 of 1.5 ns is used. Even changing the population ratio of the spin sublevels of ρ_{+1}/ρ_0 from 1.5 to 5 does not alter the spectral pattern drastically. This model requires that the ET reaction be much faster than the longitudinal relaxation of $^3\text{Xn}^*$. The diffusion controlled rate constants under the mixed solvent conditions are tabulated in Table 1. For a 60% solution of cyclohexanol, the pseudo first order rate constant of this ET reaction is $1.8 \times 10^7 \text{ s}^{-1}$. The longitudinal relaxation time (T_1) of $^3\text{Xn}^*$ reported was 5.6 ns in 2-propanol at room temperature.³² This T_1 value may change a little in the mixed solvents, but the value may be the order of 10^{-8} s. These parameters imply that the ET must be much faster than that of diffusion controlled reaction. The necessary conditions of this model are (1) quick and efficient ET and (2) slow revolution of the RIP. To meet the first of these conditions, long distance (1 nm or longer) efficient ET between $^3\text{Xn}^*$ and DEA is needed. There must be a solvent mediated long-distance ET reaction due to an effect

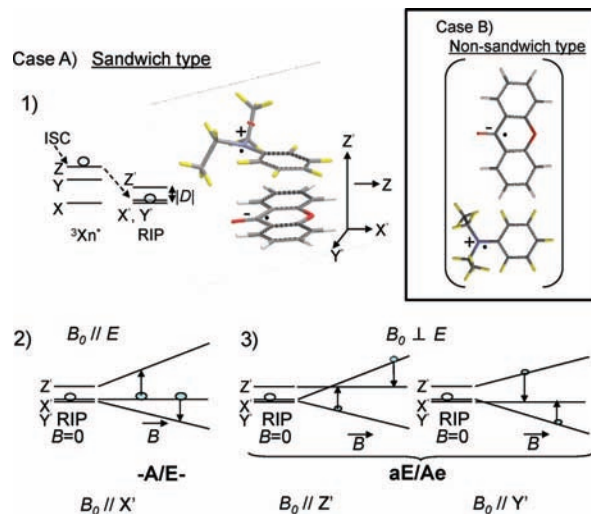


Figure 6. Case A: the sandwich type model configuration. (1) Transfer of the spin polarization from $^3\text{Xn}^*$ to the RIP. (2 and 3) diagrams of the spectral pattern at the canonical points in the case of $B_0 \parallel E$ and $B_0 \perp E$, respectively. Case B (inset): the nonsandwich type model configuration, providing the same spectral pattern to Case A (see text).

Case C) Non-sandwich type

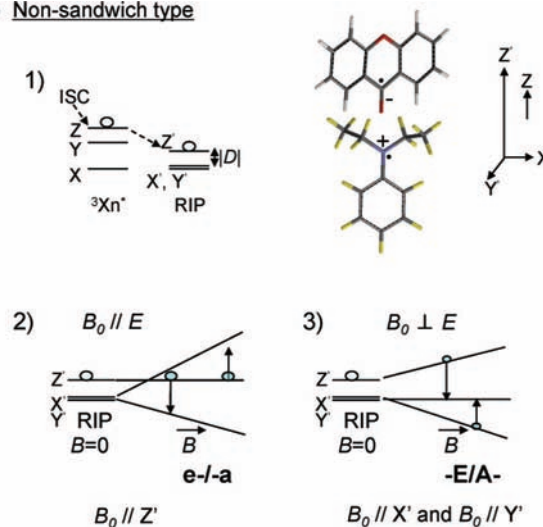


Figure 7. Case C: the nonsandwich type model configuration. (1) Transfer of the spin polarization from $^3\text{Xn}^*$ to the RIP. (2 and 3) diagrams of the spectral pattern at the canonical points in the case of $B_0 \parallel E$ and $B_0 \perp E$, respectively (see text).

such as a superexchange interaction between $^3\text{Xn}^*$ and DEA. In the case of alcohol solution at room temperature, an ET rate much faster than 10^{10} s^{-1} is expected, even at a distance of 1 nm.^{33,34} At the concentrations of DEA used, the average distance between $^3\text{Xn}^*$ and DEA is *ca.* 3 nm or less. Therefore, only the molecules closely located may react and contribute to the MPS. For condition (2), quick reorientation of the solvent molecules takes place immediately after the ET, and a huge aggregate is constructed. The free rotation of the RIP must then be frozen, and the spin d–d interaction can be observed because of no averaging of the anisotropic interaction.

II. Model of Restrained Molecular Motion. Figure 6 and Figure 7 show three possible configuration models of the RIP where the definition of X' , Y' and Z' is the same as for the previous model.

Case A. If the configuration of the RIP is face-to-face sandwich-like at the beginning (Figure 6-1), the population of

TABLE 2: ESR Spectral Pattern^a

model I	$B_0 \parallel E$	$B_0 \perp E$
	e A/E a	a E/A e
model II	$B_0 \parallel E$	$B_0 \perp E$
sandwich type (case A)	–A/E–	a E/A e
nonsandwich type (case B)	–A/E–	a E/A e
nonsandwich type (case C)	e–/–a	–E/A–
combined	e A/E a	a E/A e
total E	e E/E e	e E/E e
model I or II + total E	e A ^{*a} /E ^{–*a}	– ^{*a} E/A ^{*ae}

^a Asterisk indicates hidden or distorted by the total E component

Z sublevel of $^3\text{Xn}^*$ is exclusively transferred to the X' axis of the RIP. Let us consider the situation in which the Xn is efficiently excited by the polarized light. In the case of $B_0 \parallel E$ where the carbonyl group is aligned parallel to the magnetic field, an –A/E– spectrum is predicted (Figure 6-2). Here, a hyphen indicates the absence of spin polarization at a given canonical point. In the case of $B_0 \perp E$, where the carbonyl group aligned perpendicular to the field, an aE/Ae spectrum is predicted (two possible principal direction cases, $B_0 \parallel Y'$ and $B_0 \parallel Z'$, are depicted in Figure 6-3). Since the spin polarized spectral components of the outer field transitions, a and e, are in principle weak, the spectral pattern is emphasized for the inner field transitions.

Two other models, case B and C, where the configuration is not face-to-face, are shown in the inset of Figures 6 and Figure 7, respectively.

Case B. In this model, DEA⁺ aligns to the direction perpendicular to the carbonyl group. The expected spectral pattern is the same as that of the face-to-face arrangement.

Case C. In this model, DEA⁺ aligns to the direction of carbonyl group of Xn⁺. The population of the Z sublevel of $^3\text{Xn}^*$ is transferred to the Z' sublevel of the RIP as shown in Figure 7-1. For the cases of $B_0 \parallel E$ and $B_0 \perp E$, e–/–a and –E/A– spectral patterns are anticipated (Figure 7, parts 2 and 3).

The detailed structure of the spin-polarized spectra shown in Figure 3 cannot be explained by any of these fixed configuration models. This suggests that complex formation and/or fixed configuration in the ground-state of Xn and DEA is unlikely. Let us consider the case of a random configuration of $^3\text{Xn}^*$ and DEA. In general, for such a random configuration, the MPS of the spectral transition is not expected. However, the signal intensity of the spectrum is induced by the spin-polarization transfer from $^3\text{Xn}^*$ to the RIP formed by ET. Since the spin-polarization at these four canonical points is characteristic, we can, in principle, qualitatively predict the polarization pattern at the canonical points of this randomly configured RIP by simply combining the patterns of the three fixed configurations. Table 2 shows the combination of these three configurations, which are the three possible dimensional configurations based on the carbonyl axis of Xn, under the condition of the MPS experiment. As indicated in table 2, the predicted spectral pattern is in good agreement with the structure marked by asterisks in figure 3. This result and the above assumption suggest that fast ET may take place between randomly oriented $^3\text{Xn}^*$ and DEA in this model. Therefore, the efficient ET, mediated by solvent molecules, and slow revolution of the RIP employed in model I are also necessary in this model. The rotational correlation time of a small-sized molecule like Xn can be estimated to be less than 10^{-10} s at the experimental viscosity of $\eta = 9.24$. This

means that the reaction must have a rate much greater than 10^{10} s⁻¹ or no MPS can be expected. This requirement for very rapid electron transfer is difficult to meet, which means that this mechanism is unlikely. If the motion of $^3\text{Xn}^*$ is frozen by the formation of an aggregate with solvent molecules, the possibility of sufficiently rapid electron transfer is increased.

The data analysis and discussion above indicate that model I is more plausible than model II. These experiments also suggest that ET between the donor and the acceptor is mediated by the solvent molecules and that the d–d interaction indicates the highest probable ET distance of two randomly oriented molecules. A detailed consideration of the spin polarization transfer at early time and the spectral growth at late time will appear elsewhere.

Conclusion

The tr-ESR spectrum of the RIP formed in the photolysis of Xn and DEA in viscous solution of the mixture of 2-propanol and cyclohexanol reveals the triplet state of the RIP of Xn⁻ and DEA⁺. The spectrum is emissively biased due to the influence of the spin polarization from $^3\text{Xn}^*$. Immediately after laser photolysis, the spin-polarized RIP spectrum exhibits MPS. This suggests that the ET reaction is faster than the longitudinal relaxation of $^3\text{Xn}^*$ or much faster than the tumbling motion of the $^3\text{Xn}^*$. The quick formation of a huge aggregate with solvent molecules obstructs the free revolution of the RIP. The MPS spectra also indicate that only closely located molecules react by the solvent-mediated ET to form the RIP.

Acknowledgment. This work has been supported by the grant of Japan Society for the Promotion of Science 196139 (JSPS). The authors are grateful to Center for Instrumental Analyses for the support in obtaining the tr-ESR data.

References and Notes

- (1) Igarashi, M.; Sakaguchi, Y.; Hayashi, H. *Chem. Phys. Lett.* **1995**, *243*, 545.
- (2) Murai, H.; Matsuyama, A.; Iwasaki, Y.; Enjo, E.; Maeda, K.; Azumi, T. *Appl. Magn. Reson.* **1997**, *12*, 411.
- (3) Murai, H.; Matsuyama, A.; Ishida, T.; Iwasaki, Y.; Maeda, K.; Azumi, T. *Chem. Phys. Lett.* **1997**, *264*, 619.
- (4) Matsuyama, A.; Maeda, K.; Murai, H. *J. Phys. Chem. A* **1999**, *103*, 4137.
- (5) Matsuyama, A.; Murai, H. *J. Phys. Chem. A* **2002**, *106*, 2227.
- (6) Matsuyama, A.; Murai, H. *Riken Rev.* **2002**, *44*, 100.
- (7) Gorelik, E. V.; Lukzen, N. N.; Sagdeev, R. Z.; Murai, H. *Phys. Chem. Chem. Phys.* **2003**, *5*, 5438.
- (8) Ishigaki, A.; Murai, H. *Chem. Phys. Lett.* **2006**, *426*, 81.
- (9) Alvarado, R.; Grivet, P. J.; Igier, C.; Barcelo, J.; Rigaudy, J. *J. Chem. Soc., Faraday Trans. 2* **1977**, *73*, 844.
- (10) Regev, A.; Michaeli, S.; Cyr, M.; Sessler, J. L.; Levanon, H. *J. Phys. Chem.* **1991**, *95*, 9121.
- (11) Judeikis, H. S.; Siegel, S. *J. Phys. Chem.* **1970**, *74*, 1228.
- (12) Michaeli, A.; Regev, A.; Mazur, Y.; Feitelson, J.; Levanon, H. *J. Phys. Chem.* **1993**, *97*, 9154.
- (13) Berg, A.; Galili, T.; Kotlyar, A. B.; Hazani, M.; Levanon, H. *J. Phys. Chem. A* **1999**, *103*, 8372.
- (14) El-Sayed, M. A.; Siegel, S. *J. Chem. Phys.* **1966**, *44*, 1416.
- (15) Adrian, F. J.; Bohandy, J.; Kim, B. F. *J. Chem. Phys.* **1984**, *81*, 3805.
- (16) Borovykh, I. V.; Proskuryakov, I. I.; Klenina, I. B.; Gast, P.; Hoff, A. J. *J. Phys. Chem. B* **2000**, *104*, 4222.
- (17) Fouassier, J. P.; Rabek, J. F., Eds. *Radiation Curing in Polymer Science and Technology*; Elsevier Applied Science: London and New York, 1993; Vol. 2.
- (18) Takamori, D.; Aoki, T.; Yashiro, H.; Murai, H. *J. Phys. Chem. A* **2001**, *105*, 6001.
- (19) Murov, S. L. *Handbook of Photochemistry*, Marcel Dekker Inc.: New York, 1973.
- (20) Miyagawa, K.; I'Haya, Y. J.; Murai, H. *Nippon Kagaku Kaishi* **1989**, *8*, 1358.

(21) *Landolt-Börnstein Numerical Data and Functional Relationships in Science and Technology*; Springer-Verlag: Berlin, Heidelberg, Germany, and New York, 1977; Vol. 9.

(22) Koga, T.; Ohara, K.; Kuwata, K.; Murai, H. *J. Phys. Chem. A* **1997**, *101*, 8021.

(23) Sakaguchi, Y.; Hayashi, H.; Murai, H.; I'Haya, Y. *J. Am. Chem. Soc.* **1988**, *110*, 7479.

(24) Imamura, T.; Onitsuka, O.; Murai, H.; Obi, K. *J. Phys. Chem.* **1984**, *88*, 4028.

(25) Akiyama, K.; Tero-Kubota, S.; Ikoma, T.; Ikegami, Y. *J. Am. Chem. Soc.* **1994**, *116*, 5324.

(26) Itoh, K.; Hayashi, H.; Nagakura, S. *Mol. Phys.* **1969**, *17*, 561.

(27) Gastilovich, E. A. *Chem. Phys.* **2003**, *292*, 81.

(28) Pownall, Henry J. *J. Am. Chem. Soc.* **1971**, *93*, 6429.

(29) Yamamoto, Y.; Murai, H.; I'Haya, Y. *J. Chem. Phys. Lett.* **1984**, *112*, 559.

(30) Murai, H.; Yamamoto, Y.; I'Haya, Y. *J. Can. J. Chem.* **1991**, *69*, 1643.

(31) Murai, H.; Minami, M.; I'Haya, Y. *J. Chem. Phys.* **1994**, *101*, 4514.

(32) Ohara, K.; Murai, H.; Kuwata, K. *Bull. Chem. Soc. Jpn.* **1992**, *65*, 1672.

(33) Ponce, A.; Gray, H. B.; Winkler, J. R. *J. Am. Chem. Soc.* **2000**, *122*, 8187.

(34) Kobori, Y.; Yago, T.; Akiyama, K.; Tero-Kubota, S.; Sato, H.; Hirata, F.; Norris, J. R. *J. Phys. Chem. B*, **2004**, *108*, 10226.

JP807088Q